Redox Biology 16 (2018) 21–31

Contents lists available at ScienceDirect

Redox Biology

journal homepage: www.elsevier.com/locate/redox

Differential effects of short chain fatty acids on endothelial Nlrp3 inflammasome activation and neointima formation: Antioxidant action of butyrate

Xinxu Yuan, Lei Wang, Owais M. Bhat, Hannah Lohner, Pin-Lan Li*

Department of Pharmacology and Toxicology, Virginia Commonwealth University, School of Medicine, Richmond, VA, USA

ARTICLE INFO

Keywords:
Arterial endothelium
Short chain fatty acids
Inflammation
Neointima
Atherosclerosis

ABSTRACT

Short chain fatty acids (SCFAs), a family of gut microbial metabolites, have been reported to promote preservation of endothelial function and thereby exert anti-atherosclerotic action. However, the precise mechanism mediating this protective action of SCFAs remains unknown. The present study investigated the effects of SCFAs (acetate, propionate and butyrate) on the activation of Nod-like receptor pyrin domain 3 (Nlrp3) inflammasome in endothelial cells (ECs) and associated carotid neointima formation. Using a partial ligated carotid artery (PLCA) mouse model fed with the Western diet (WD), we found that butyrate significantly decreased Nlrp3 inflammasome formation and activation in the carotid arterial wall of wild type mice ($Asc^{+/+}$), which was comparable to the effect of gene deletion of the adaptor protein apoptosis-associated speck-like protein gene ($Asc^{-/-}$). Nevertheless, both acetate and propionate markedly enhanced the formation and activation of the Nlrp3 inflammasome as well as carotid neointima formation in the carotid arteries with PLCA in $Asc^{+/+}$, but not $Asc^{-/-}$ mice. In cultured ECs (EOMA cells), butyrate was found to significantly decrease the formation and activation of Nlrp3 inflammasomes induced by 7-ketocholesterol (7-Ket) or cholesterol crystals (CHC), while acetate did not inhibit Nlrp3 inflammasome activation induced by either 7-Ket or CHC, but itself even activated Nlrp3 inflammsomes. Mechanistically, the inhibitory action of butyrate on the Nlrp3 inflammasome was attributed to a blockade of lipid raft redox signaling platforms to produce $O2^{\bullet-}$ upon 7-Ket or CHC stimulations. These results indicate that SCFAs have differential effects on endothelial Nlrp3 inflammasome activation and associated carotid neointima formation.

1. Introduction

Short chain fatty acids (SCFAs) are saturated fatty acids characterized by an aliphatic carbon chain length of at most eight carbon atoms [1], which are mainly produced in a fermentation process by microbiota in the colon and the distal small intestine from resistant starch or dietary fiber [2,3]. Acetate, propionate, and butyrate (Fig. 1A) are the predominant SCFAs in the proximal regions of the large intestine in humans and rodents, and are present at high mM levels [3–7]. Once produced, SCFAs are readily absorbed by enterocytes of the intestines [8]. It has been reported that the majority of absorbed SCFAs are used as an energy source, but a portion of these absorbed fatty acids is released via the basolateral membrane to the hepatic portal vein and then reaches the systemic circulation. After reaching systemic circulation, low concentration SCFAs will affect the biological activities of various peripheral tissues [9,10]. There is evidence that SCFAs are able to have anti-inflammatory effects on the digestion system and other tissues to attenuate the development of related inflammatory diseases including inflammatory bowel disease (IBD), colon cancer, obesity and type 1 and 2 diabetes mellitus [11–15]. However, the effects of SCFAs on various cardiovascular diseases associated with inflammation remain poorly understood.

The Nlrp3 inflammasome, an intracellular inflammatory machinery, is a well-characterized type of inflammasome in mammalian cells so far. It consists of a large cytosolic multiprotein complex formed mainly by the sensor protein, Nod-like receptor pyrin domain 3 (Nlrp3), the adaptor protein apoptosis-associated speck-like protein (*Asc*), and the pro-inflammatory caspase-1 [16–19]. Upon pathological stimulations, Nlrp3 inflammasome components are assembled leading to the autocatalysis and activation of caspase-1, which is responsible for the maturation of pro-inflammatory cytokines, such as bioactive interleukin-1β (IL-1β) and interleukin-18 (IL-18) [20,21]. The Nlrp3 inflammasome has been implicated in the pathogenesis of various metabolic diseases including diabetes mellitus, gout, silicosis, acute myocardial infarction,

* Correspondence to: Department of Pharmacology & Toxicology, Medical College of Virginia Campus, Virginia Commonwealth University, Richmond, VA 23298, USA.
E-mail address: pin-lan.li@vcuhealth.org (P.-L. Li).

https://doi.org/10.1016/j.redox.2018.02.007
Received 11 January 2018; Received in revised form 2 February 2018; Accepted 12 February 2018
Available online 13 February 2018

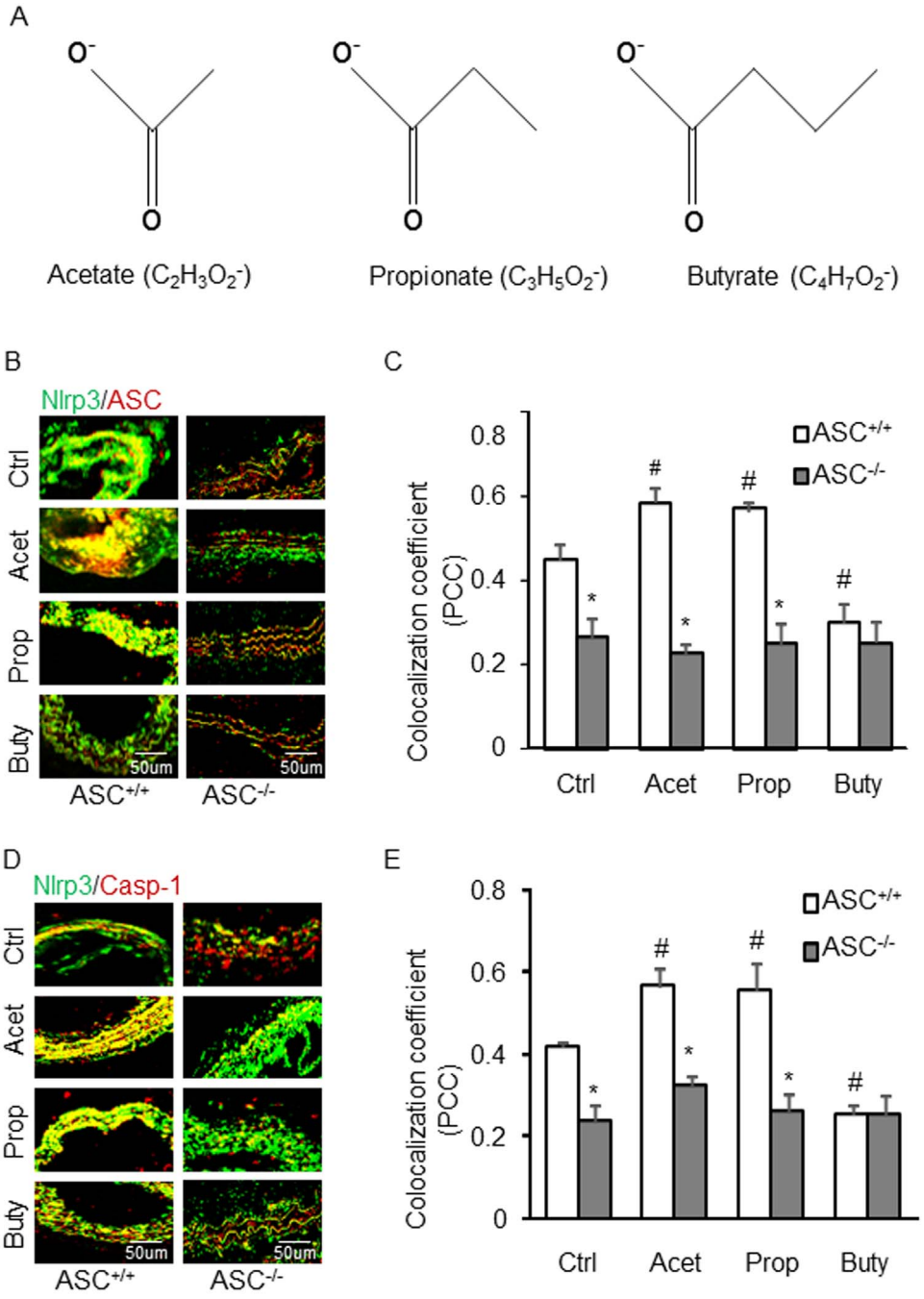

Fig. 1. Effects of SCFAs on the formation of Nlrp3 inflammasome in the partial ligated carotid artery of mice. A. Representative schematic of three short chain fatty acid structures. B. Representative fluorescent confocal microscopic images showing the colocalization of Nlrp3 with *Asc*. C. Summarized data showing Pearson correlation coefficient (PCC) of Nlrp3 with *Asc* (n = 5). D. Representative fluorescent confocal microscopic images showing the colocalization of Nlrp3 with Caspase-1. E. Summarized data showing Pearson correlation coefficient (PCC) of Nlrp3 with Caspase-1 (n = 5). Data are expressed as means ± SEM. * $p < 0.05$ vs. $Asc^{+/+}$ group; # $p < 0.05$ vs. Ctrl (control).

and liver toxicity [17,20,22,23]. With respect to the effects of SCFAs, Wang et al. reported that the Nlrp3 inflammasome was activated by sodium butyrate in db/db mice [24], while Ho et al. demonstrated that bamboo vinegar decreases inflammatory mediator expression and Nlrp3 inflammasome activation by inhibiting reactive oxygen species (ROS) generation and protein kinase C-α/δ activation both in vitro and in vivo [25]. There is evidence that ketone bodies, β-hydroxybutyrate (BHB), but not acetoacetate (AcAc) or the structurally related SCFAs, butyrate and acetate, suppress activation of the Nlrp3 inflammasome in response to urate crystals, ATP and lipotoxic fatty acids [25,26]. All these studies have suggested that SCFAs may target Nlrp3 inflammasome formation and activation to produce corresponding biological action. Since activation of the Nlrp3 inflammasome has been reported to be involved in coronary endothelial dysfunction and atherosclerosis [27], we hypothesized that the endothelial Nlrp3 inflammasome may be a target for SCFAs to alter endothelial function and neointima formation.

In the present study, we used partial carotid ligation (PLCA) as a model of acutely induced disturbed flow leading to rapid endothelial dysfunction and atherosclerosis [28]. This model is considered as an appropriate animal model for studying endothelial injury associated with inflammatory response such as macrophage infiltration, smooth muscle proliferation, and extracellular matrix reorganization and resulting remodeling of LCA with intima-media-adventitial thickening

(IMT) [29]. In recent studies, our laboratory also showed that PLCA is an ideal model for studies on the formation and activation of Nlrp3 inflammasomes, which consequently lead to arterial inflammation and endothelial dysfunction in mice. As one component of Nlrp3 inflammasome, Asc expression increased in the neointima after vascular injury in mice [30], and Nlrp3 inflammasome formation and activation were blocked in *Asc* knock-out mice [31]. Therefore, the present study tested the effects of SCFAs on Nlrp3 inflammasomes using PLCA-induced neointeima formation model with wild type mice ($Asc^{+/+}$) and Asc knock-out mice ($Asc^{-/-}$), where $Asc^{-/-}$ was considered as a positive control for confirmation of Asc associated inflammasome is involved in the effects of SCFAs.

The present study was designed to analyze the effects of SCFAs (acetate, propionate and butyrate) on Nlrp3 inflammasome formation and activation in endothelial cells. We first examined whether SCFAs had inhibitory effects on Nlrp3 inflammasome formation and activation in vivo using a partially ligated carotid artery (PLCA) model in wild type mice on the Western diet (WD) [16], which was compared with the effects of *Asc* gene knockout ($Asc^{-/-}$) mice. Then, we further explored the mechanisms by which SCFAs alter Nlrp3 inflammasomes upon stimulations of atherosclerotic stimuli such as 7-ketocholesterol (7-Ket) and cholesterol crystals (CHC). Our results demonstrated that different SCFAs had differential effects on the Nlrp3 activation and arterial neointima formation. Among SCFAs, butyrate was shown to have a promising beneficial effect, which can be exploited as a new source for the development of therapeutic strategies for atherosclerotic diseases.

2. Materials and methods

2.1. Mice

All animal experiments were performed in accordance with the National Institutes of Health guidelines for the care and use of laboratory animals. The protocols were approved by the Institutional Animal Care and Use Committee of Virginia Commonwealth University. Eight-week-old male and female C57BL/6J *Asc* wild-type ($Asc^{+/+}$) and *Asc* knock-out ($Asc^{-/-}$) mice were used in the current study. Mice were maintained in a controlled environment of 20 °C and 40–50% humidity, with a 12-h light/dark cycle. $Asc^{+/+}$ and $Asc^{-/-}$ mice were separated into 4 groups randomly and fed with the WD for 30 days.

2.2. Partial ligated carotid artery

Partial ligated carotid artery (PLCA) surgery was performed as previously reported by others [29,32–35]. Briefly, mice were anaesthetized with 2% isoflurane inhalation for 5 min and epilated in the neck, then continued being anaesthetized through a nose cone. A ventral midline incision was made in the neck disinfected with 70% ethanol, and then the muscle layers were separated with curved forceps to expose the left carotid artery after blunt dissection. The external carotid, internal carotid and occipital artery were ligated with a piece of 6.0 silk suture, while the superior thyroid artery was left intact, which provided the sole source for blood circulation. The right carotid artery was not ligated and served as an internal control. After closing the incision and disinfection, the mice were kept on a heating pad until they gained consciousness. Two days before PLCA, mice were injected intraperitoneally with 500 mg/kg acetate sodium, propionate sodium or butyrate sodium once a day for 17 days. The dose of these SCFAs chosen to be used in these animal protocol were based on our preliminary studies in cells, which was calculated from a concentration mostly effective in vitro into in vivo doses (see Figs. S1–S3 in Supplementary material). These doses of SCFAs used were also consistent from some previous studies [36,37]. After two weeks of PLCA, mice were sacrificed and both of their carotid arteries were perfused and isolated for frozen sections and paraffin sections. The slides were used for immunohistochemistry, dual fluorescence staining and confocal analysis respectively.

2.3. Immunofluorescence staining

Cells cultured in 8-well plates or coronary artery on frozen slides were rinsed 2–3 times for 5 min with PBS and fixed in 4% paraformaldehyde in PBS for 15 min. After being washed 2–3 times with PBS for 5 min, the samples were permeabilized with 0.1% Triton X-100 in PBS for 10 min and were washed 2–3 times for 5 min with PBS. Then samples were incubated with a primary antibody overnight at 4 °C followed by incubation with either Alexa-488- or Alexa-555-labeled secondary antibody for 1 h at room temperature in the dark room. Finally, the slides were mounted with mounting medium with DAPI and sealed with nail polish for taking pictures using a confocal laser scanning microscope (Fluoview FV1000; Olympus, Tokyo, Japan). Cell or tissue specific staining intensity was measured and analyzed with Image J software. The colocalization of Nlrp3 with Asc or caspase-1 was analyzed by the Image Pro Plus version 6.0 software (Media Cybernetics, Bethesda, MD). These summarized colocalization efficiency data were expressed as Pearson correlation coefficient (PCC) as described previously [32,38].

2.4. Immunohistochemistry

The carotid arteries were embedded with paraffin and 5 μm slices were cut from the embedded blocks. After heat-induced antigen retrieval, slides were incubated with primary antibodies diluted in phosphate-buffered saline (PBS). Anti-IL-1β antibodies were used in this study. After incubation with primary antibody overnight, the sections were washed in PBS and incubated with biotinylated IgG (1:250) for 1 h and then with streptavidin-HRP for 30 min at room temperature. Then, 50 μl of DAB was added to each section and stained for 1–5 min. After washing, the slides were counterstained with hematoxylin for 2 min. The slides were then mounted and observed under a microscope in which photos were taken [39].

2.5. In situ analysis of caspase-1 activity

Caspase-1 activity was performed as we described previously [19]. This assay used Fluorescent Labeled Inhibitor of Caspases (FLICATM) probes (ImmunoChemistry Technologies, LLC, Bloomington, MN, USA) to label activated caspase-1 enzyme in the coronary arterial endothelium. The FLICA probes are comprised of a caspase-1 recognition sequence tyrosine-valine-alanine-aspartic acid (YVAD) that binds to active caspase-1, a fluoromethyl ketone (FMK) moiety that results in irreversible binding with the enzyme, and a fluorescent tag FAM (carboxyfluorescein) reporter. After entering the cells, the FLICA reagent FAM-YVAD-FMK becomes covalently coupled to the active caspase-1, while any unbound FLICA reagent diffuses out of the cell and is washed away. The remaining green fluorescent signal is a direct measure of the active caspase-1 enzyme activity in the cell or tissue samples. To detect caspase-1 activity in the coronary arterial endothelium, frozen artery section slides were first fixed in acetone and incubated overnight at 4 °C with sheep anti-vWF (1:200; Abcam). These slides were then co-stained with fluorescence conjugated anti-sheep secondary antibody and FLICA reagent (1:10) from a FLICATM Caspase 1 Assay Kit (Immunochemistry Technologies, LLC) for 1.5 h. at room temperature, washed, mounted, visualized and analyzed by confocal microscopy as described above. Colocalization was analyzed by Image Pro Plus software. The colocalization coefficient was represented by PCC.

2.6. Cell culture

The mouse EC cell line also known as EOMA cells was purchased from ATCC, which isolated originally from mouse hemangioendothelioma. Passage 5–10 EOMA cells were cultured in Dulbecco's modified

Eagle's medium (DMEM, Gibco), supplemented with 10% FBS (Gibco) and 1% penicillin–streptomycin (Gibco) in humidified 100% air and 5% CO_2 mixture at 37 °C. 2×10^5 cells were prepared in 6-well plates overnight, 80–90% confluence cells were treated with 5 mM acetate sodium, 5 mM propionate sodium or 1 mM butyrate sodium for 2 h before being treated with or without 7-Ket or CHC for 24 h as described previously [27].

2.7. Western blot analysis

Western blot analysis was performed as we described previously [40]. Briefly, total protein was extracted using lysis buffer with protein inhibitor after being washed in cold PBS. Protein concentrations were measured and resuspended to 2 μg/μl. Cell lysates were run on a SDS-PAGE gel at a voltage of 100 V for 2 h, transferred into polyvinylidene difluoride membrane at voltage of 100 V for 1 h, and blocked with 5% non-fat milk in TBST buffer for 30 min. Then, the membrane was incubated with primary antibodies against, pro-caspase-1, or cleaved caspase-1 (1:500 dilution, Santa Cruz) overnight at 4 °C, followed by incubation with a secondary antibody labeled with HRP for 1 h at room temperature. The membrane was developed with Kodak Omat film after being washed 3 times with TBST. β-actin (1:8000 dilution, Santa Cruz) was reported to serve as a loading control. The intensity of the bands was quantified using ImageJ 6.0 (NIH, Bethesda, MD, USA) [41].

2.8. ELISA analysis of IL-1β secretions

The culture medium was collected for IL-1β quantification with an IL-1β ELISA kit according to the manufacturer's instructions and our previous studies [42]. In brief, 100 μl of the culture medium were added to a microplate strip well and incubated for 2 h at room temperature. Then, the solution was mixed with IL-1β conjugate and incubated for another 2 h at room temperature. Thorough washes were performed between and after the two incubations. 100 μl of substrate solution was applied to generate chemiluminescence. Chemiluminescent absorbance was determined using a microplate reader at $\lambda = 450$, corrected to readings at $\lambda = 570$. The IL-1β level was quantified by relating the sample readings to the generated standard curve.

2.9. Electromagnetic spin resonance (ESR) analysis of $O_2^{\cdot-}$ production

ESR detection of $O_2^{\cdot-}$ was performed as we previously described [43]. Briefly, ESR spectrometric detection of $O_2^{\cdot-}$ was performed in cultured ECs and spin trapping compound. Cellular protein samples were prepared by using modified Kreb's-Hepes buffer containing deferoxamine (100 μM) and diethyldithiocarbamate (5 μM). NADPH oxisase (NOX)-dependent $O_2^{\cdot-}$ production was examined by addition of 1 mM NADPH as a substrate in 30 μg protein in the presence or absence of superoxide dismutase (800 U/mL) to produce $O_2^{\cdot-}$. Then, 10 mM $O_2^{\cdot-}$ specific spin trapping compound, 1-hydroxy-3-methoxycarbonyl-2,2,5,5-tetramethylpyrrolidine (CMH) was added to trap $O_2^{\cdot-}$. The mixture was loaded in glass capillaries and immediately analyzed for $O_2^{\cdot-}$ production kinetically for 10 min using a Miniscope MS200 ESR spectrometer (Magnettech, Germany). The ESR settings were as follows: biofield, 3350; field sweep, 60 G; microwave frequency, 9.78 GHz; microwave power, 20 mW; modulation amplitude, 3G; 4096 points of resolution; receiver gain, 100; and kinetic time, 10 min. SOD sensitive components of ESR signals were used to calculate changes in $O_2^{\cdot-}$ production or its level, which were shown as the fold changes of control.

2.10. DHE staining

Dihydroethidium (DHE) is a lipophilic cell-permeable dye that can be oxidized by $O_2^{\cdot-}$ to form ethidium bromide. It has been commonly used to detect cytosolic superoxide [44]. Upon its reaction with the superoxide anion, DHE forms a red fluorescent product, 2-hydroxyethidium [45], with maximum excitation and emission peaks at 500 and 580 nm, respectively. In brief, the unfixed cells from different groups were incubated with DHE (10 μM) in phosphate-buffered saline at room temperature for 30 min. Then, the slides were washed, fixed, mounted, and subjected to confocal microscopic analysis (Fluoview FV1000; Olympus).

2.11. Statistics

Data are presented as means ± SEM. Significant differences between and within multiple groups were examined using ANOVA for repeated measures, followed by Duncan's multiple-range test. The statistical analysis was performed by Sigmaplot 12.5 software (Systat Software, San Jose, CA, USA). $P < 0.05$ was considered statistically significant.

3. Results

3.1. Effects of SCFAs on the formation of Nlrp3 inflammasomes in the arterial wall of PLCA

We first performed in vivo animal experiments to determine whether SCFAs prevent or enhance inflammasome activation and vascular injury using a mouse model with partial ligated carotid artery. Using confocal microscopy, the co-localization of Nlrp3 vs. Asc or caspase-1, as shown in yellow color in the arterial, increased in PLCA in wild type mice, which was seen in contralateral carotid artery (not shown). This suggests the formation of Nlrp3 inflammasomes on the wall of PLCA. However, this increased Nlrp3 inflammasome formation (colocalization of its components) was not seen in the wall of PLCA of *Asc*$^{-/-}$ mice (Figs. 1B and 1C). Surprisingly, we found that both acetate and propionate markedly increased the formation of this Nlrp3 inflammasome in PLCA wall of *Asc*$^{+/+}$ mice, but they had no effect in *Asc*$^{-/-}$ mice. However, butyrate almost completely blocked the formation of NRLP3 inflammsomes in PLCA wall of Asc$^{+/+}$, which was similar to that observed in *Asc*$^{-/-}$ mice. These results were summarized in Figs. 1C and 1E, and they suggest that administration of acetate or propionate promote vascular injury in the PLCA model, but butyrate has protective effects on vascular injury in the same mouse model.

3.2. Effects of SCFAs on endothelial caspase-1 activity and IL-1β production in the arterial wall of PLCA

Corresponding to the effects of SCFAs on Nlrp3 inflammasome formation, caspase-1 activation as shown by FLICA positive staining was found in the endothelium of PLCA, acetate, and propionate markedly increased active caspase-1 levels. However, butyrate blocked endothelial caspase-1 activation in PLCA. In *Asc*$^{-/-}$ mice, PLCA did not exhibit any endothelial activation of NRLP3 inflamamsomes, and the three SCFAs had no effects on caspase-1 activation in PLCA (Figs. 2A and 2B). We also examined IL-1β production in the wall of PLCA in *Asc*$^{+/+}$ and *Asc*$^{-/-}$ mice. As shown in Fig. 3, it is clear that PLCA significantly increased IL-1β levels in the wall of PLCA of *Asc*$^{+/+}$ mice, which was enhanced by either acetate or propionate treatment. However, butyrate treated *Asc*$^{+/+}$ mice didn't show increased IL-1β production in the wall of PLCA. These alterations of IL-1β production in the wall of PLCA in *Asc*$^{+/+}$ mice could not be observed in *Asc*$^{-/-}$ mice, suggesting that arterial IL-1β production in PLCA is attributed to Asc-dependent Nlrp3 inflammasome activation.

3.3. Effects of SCFAs on the neointima formation in PLCA

The neointima formation as a major pathological change in PLCA was also analyzed in *Asc*$^{+/+}$ and *Asc*$^{-/-}$ mice. It was found that administration of acetate or propionate caused a significant increase in the neointima formation in PLCA of *Asc*$^{+/+}$ mice as compared to

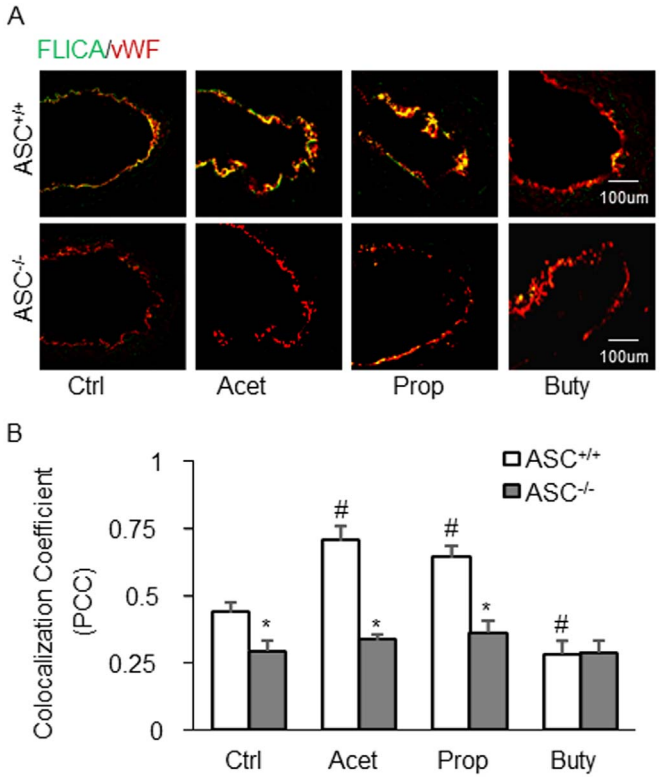

Fig. 2. Endothelial caspase-1 activity in the partial ligated carotid artery of mice. A. Representative fluorescent confocal microscopic images showing the colocalization of FLICA (a marker of caspase-1 activation) with EC marker, vWF. B. Summarized data showing Pearson correlation coefficient (PCC) of FLICA vs vWF (n = 5). Data are expressed as means ± SEM. * $p < 0.05$ vs. $Asc^{+/+}$ group; # $p < 0.05$ vs. Ctrl (control).

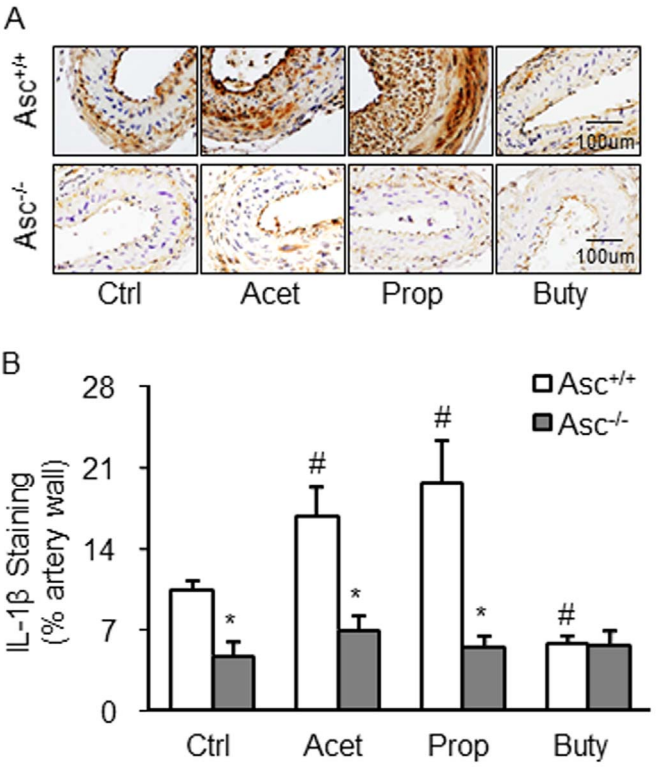

Fig. 3. IL-1β production in the Partial Ligated Carotid Artery of Mice. A. Representative microscopic images of tissue slide with immunohistochemical staining that shows IL-1β accumulation in arterial wall. B. Summarized data showing the density of IL-1β stained with selective anti-IL-1β antibody (n = 5). Data are expressed as means ± SEM. * $p < 0.05$ vs. $Asc^{+/+}$ group; # $p < 0.05$ vs. Ctrl (control).

vehicle-treated $Asc^{+/+}$ mice. In butyrate-treated $Asc^{+/+}$ mice, however, the neointima formation in PLCA was significantly inhibited. This neointima formation in PLCA and the enhancing effects by acetate and propionate were not observed in $Asc^{-/-}$ mice (Fig. 4A). The quantitation of a ratio of intima vs. media is summarized in Fig. 4B. It is clear that acetate and propionate significantly enhanced the ratio of intima vs. media in PLCA, which is dependent upon the activation of inflammasome because their effects were not seen in $Asc^{-/-}$ mice. However, butyrate had no effect on the ratio of intima vs. media in PLCA in both $Asc^{+/+}$ and $Asc^{-/-}$ mice.

3.4. Effects of SCFAs on the formation of Nlrp3 inflammasome in cultured ECs stimulated by 7-Ket and CHC

To explore the potential mechanisms mediating the effects of SCFAs specifically in ECs, we first examined the effects of 7-Ket and CHC on Nlrp3 inflammasome complex formation as shown by colocalization of Nlrp3 with Asc or caspase-1 in cultured ECs, which indicate the assembling of Nlrp3 inflammasome components (Figs. 5A and C). It was found that both 7-Ket and CHC significantly increased this inflammasome formation as compared to vehicle treated cells. Treatment of the cells with acetate not only significantly enhanced the Nlrp3 inflammasome (Nlrp3/Asc) formation stimulated by 7-Ket or CHC-stimulation, but also itself activated this inflammasome assembling. Propionate treatment only led to a significant decrease in Nlrp3 inflammasome formation in these cells with CHC stimulation, but not in those with 7-Ket as a proatherogenic stimulus. Interestingly, butyrate treatment had the opposite effect of acetate and propionate, which significantly inhibited Nlrp3 inflammasome formation stimulated by either 7-Ket or CHC. The colocalization of Nlrp3 with Asc or caspase-1 was summarized in Figs. 5B and D, which indicates the differential effects of the three SCFAs on the Nlrp3 inflammasome formation upon

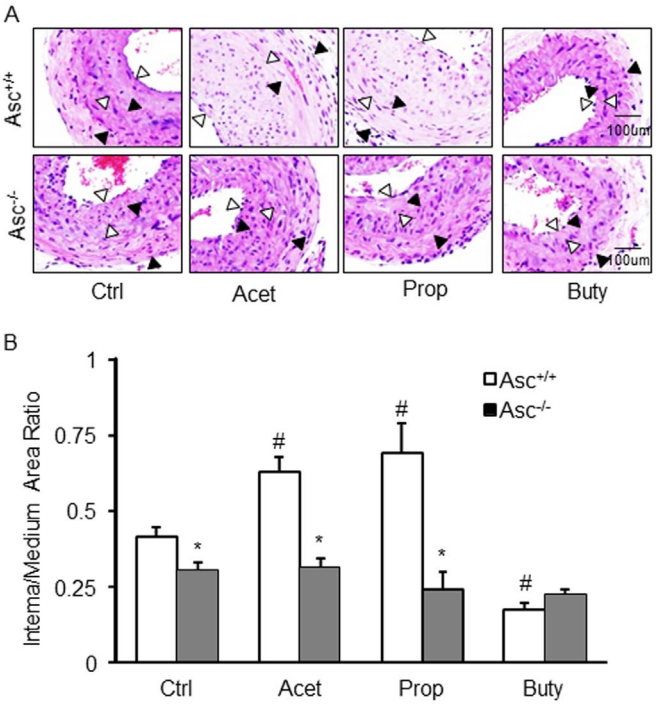

Fig. 4. Neointima formation in the partial ligated carotid artery of mice. A. HE staining showing the neointima and media in the arterial wall. AOI: the media area (black arrowheads) and the intima area (white arrowheads). B. Quantitative analysis of vascular lesions in PLCA represented by calculation of the ratio between intima and media of the arteries. * $p < 0.05$ vs. $Asc^{+/+}$ group; # $p < 0.05$ vs. Ctrl (control).

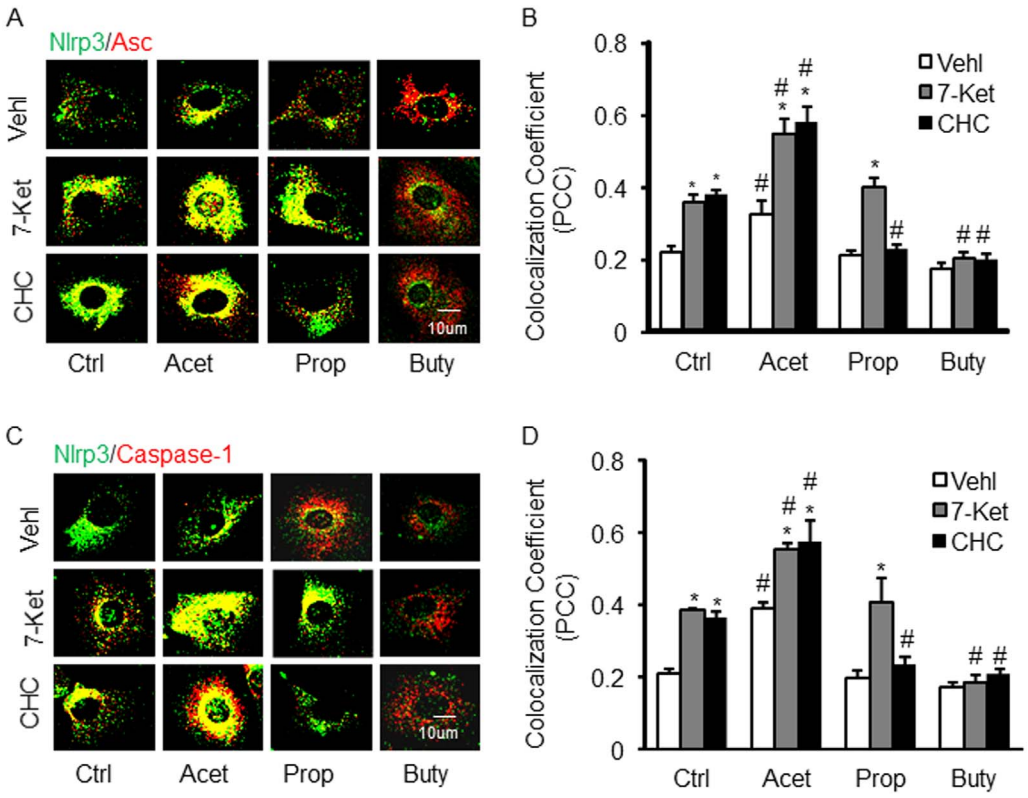

Fig. 5. Effects of SCFAs on the formation of Nlrp3 inflammasome in endothelial cells (ECs, EOMA) induced by 7-Ket and CHC. A. Representative fluorescent confocal microscopic images showing the colocalization of Nlrp3 with *Asc*. B. Summarized data showing Pearson correlation coefficient (PCC) of Nlrp3 with *Asc* (n = 5). *C.* Representative fluorescent confocal microscopic images showing the colocalization of Nlrp3 with caspase-1. D. Summarized data showing PCC of Nlrp3 with caspase-1 (n = 5). Data are expressed as means ± SEM. * $p < 0.05$ vs. Vehl group; # $p < 0.05$ vs. Ctrl. Ctrl: control; 7-Ket: 7-ketocholesterol; CHC: cholesterol crystals; Vehl: vehicle; Acet: acetate; Prop: propionate; Buty: butyrate.

7-Ket and CHC in ECs.

3.5. Effects of SCFAs on the activation of Nlrp3 inflammasome induced by 7-Ket and CHC in ECs

We also examined the effects of SCFAs on the activation of Nlrp3 inflammasomes. It was found that the level of cleaved caspase-1 in ECs, which is reported as a parameter of Nlrp3 inflammasome activation in a variety of cell types, was significantly increased as shown by enhanced production of cleaved caspase-1 as compared to vehicle-treated cells. Acetate significantly increased cleaved caspase-1 levels and augmented 7-Ket-stimulated elevation of this cleaved caspase-1 in ECs. However, propionate had no effects on 7-Ket-stimulated increase in caspase-1 levels, while butyrate even reduced this 7-Ket-stimulated activation of caspase-1 (Figs. 6A and B). In CHC stimulated cells, the three SCFAs had similar action patterns to those observed in 7-Ket-stimulated cells except propionate blocked CHC-induced increase in cleaved caspase-1 level (Figs. 6C and D).

By quantitation of IL-1β production and direct analysis of caspase-1 activity, we further confirmed the effects of SCFAs on the activation of Nlrp3 inflammasome in ECs. As shown in Fig. 7A, acetate was found to significantly increase IL-1β production in the supernatant of cultured ECs and to enhance 7-Ket- and CHC-stimulated production of IL-1β. Propionate had no effects on 7-Ket-stimulated production of IL-1β, but inhibited CHC-stimulated increase in IL-1β production. Butyrate almost completely abolished both 7-Ket and CHC-stimulated production of IL-1β in these ECs. Fig. 7B shows the effects of the three different SCFAs on the caspase-1 activity in ECs with or without 7-Ket or CHC stimulations. Similar to quantitation of IL-1β, acetate significantly increased caspase-1 activity and enhanced 7-Ket- and CHC-stimulated activation of this enzyme activity. Propionate had no effects on 7-Ket-increased caspase-1 activity, but inhibited CHC-enhanced caspase-1 activity. Butyrate was found to completely block both 7-Ket and CHC-induced enhancement of caspase-1 activity.

3.6. Effects of butyrate associated with suppression of lipid raft redox signaling platform activation

Given previous reports about the beneficial action of SCFAs in a number of cardiovascular diseases, we were particularly interested in the mechanisms mediating the inhibitory effects of butyrate on Nlrp3 inflammasome formation and activation. Since recent studies showed that the lipid raft (LR) redox signaling platforms were involved in Nlrp3 inflammasome activation [46,47], we determined the contribution of LR redox signaling platform formation and activation induced by 7-Ket and CHC. In these experiments, ECs were stained with Alexa Fluor 488-labeled CTXB (a LR marker) and anti-gp91 or anti-p47 antibody [NOX subunits] to detect clustering of LRs with both NOX subunits, an indicator of LR redox signaling platform formation or activation. It was found that butyrate prevented the increases in LR clustering with gp91 (Fig. 8A and B) or p47 (Fig. 8C and D) upon stimulations of 7-Ket or CHC, as shown by the yellow patch formation on the ECs membrane detected by confocal microscopy. This effect of butyrate was similar to that produced by a ROS scavenger, N-acetyl-L-cysteine (NAC, at 10 μM, Sigma) (Fig. 8A–D). We also performed ESR spectromentry and DHE staining to measure $O_2^{\bullet-}$ production. It was found that 7-Ket or CHC-induced $O_2^{\bullet-}$ production in ECs was blocked by butyrate, which was similar to the effect of NAC in the same cell preparations with 7-Ket or CHC stimulations (Fig. 8E and F).

4. Discussion

The development of cardiovascular diseases is often attributable to the early loss of endothelial functions caused by imbalances in lipid and glucose metabolism and by other danger factors such as cytokines, chemokines and damage-associated molecular patterns (DAMPs) [48]. The cellular or plasma lipid imbalances can result in a low-grade non-sterile inflammatory state of the affected endothelium, causing macrophage foam cell formation and fat-rich lipoproteins to accumulate in the subendothelial space and ultimately resulting in arterial sclerosis

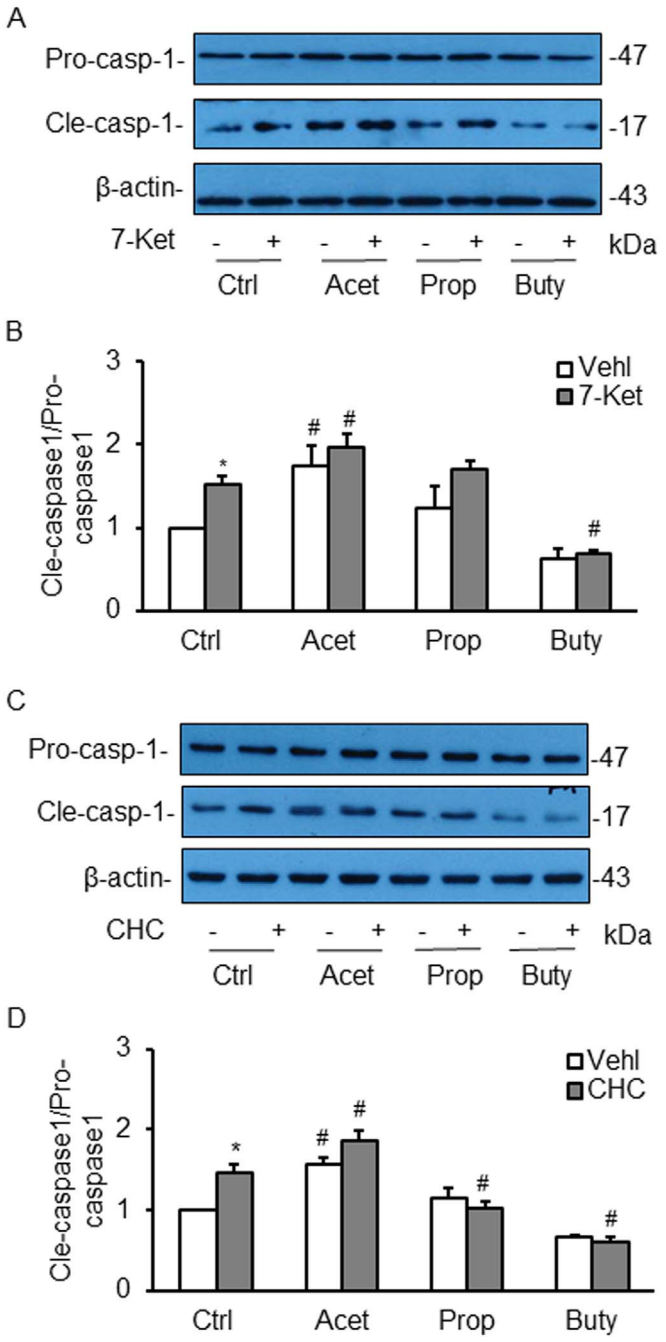

Fig. 6. Effects of SCFAs on the activation of Nlrp3 inflammasome detected in ECs induced by 7-Ket and CHC. A. Representative Western blot gel documents showing the expression of pro-caspase-1 and cleaved caspase-1 induced by 7-Ket. B. Summarized Data showing the ratio of cleaved caspase-1 with pro-caspase-1 induced by 7-Ket (n = 5). *C.* Representative Western blot gel documents showing the expression of pro-caspase-1 and cleaved caspase-1 induced by CHC. D. Summarized data showing the ratio of cleaved caspase-1 with pro-caspase-1 induced by CHC (n = 5). Data are expressed as means ± SEM. * $p < 0.05$ vs. Vehl group; # $p < 0.05$ vs. Ctrl.

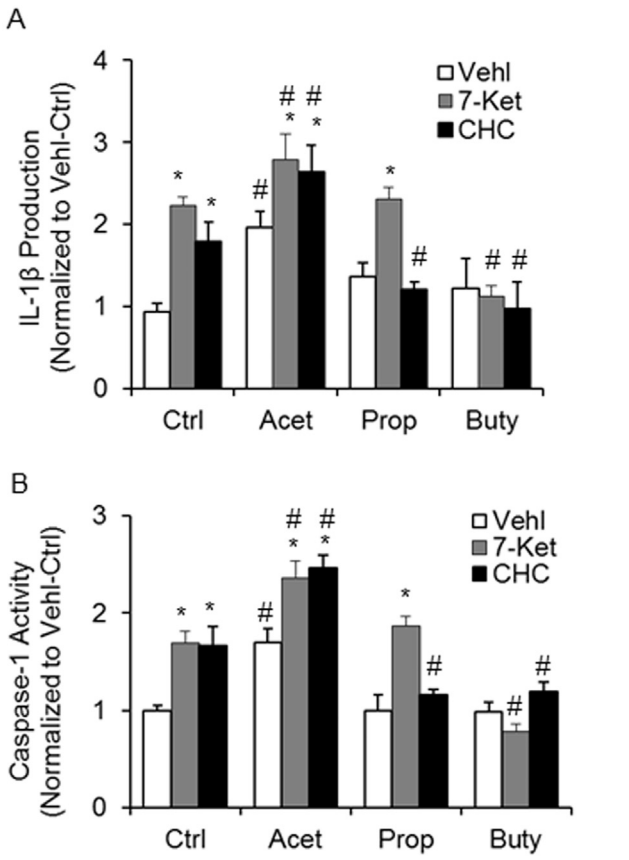

Fig. 7. Effects of SCFAs on Caspase-1 activity and IL-1β production stimulated by 7-Ket and CHC. A. Summary data showing caspase-1 activity (n = 5). B. Summarized data showing IL-1β production (*n = 5).* Data are expressed as means ± SEM. * $p < 0.05$ vs. Vehl group; # $p < 0.05$ vs. Ctrl.

and plaque formation. Recently, we and others have reported that endothelial Nlrp3 inflammasome activation may be an important triggering mechanism by which endothelial injury in response to atherogenic stimuli activates vascular inflammation and also induces uncanonical detrimental effects on the endothelium itself and other cells leading to atherosclerosis [19,27,32,49]. It has been indicated that the Nlrp3 inflammasome may be an important therapeutic target for treatment and prevention of atherosclerosis. The present study tested the potential effects of SCFAs on endothelial Nlrp3 inflammasome activation upon stimulation of atherogenic stimuli such as 7-Ket and CHC because these fatty acids were reported to possibly mediate the beneficial action of the diet with high fibers on cardiovascular diseases [10,50–52]. We surprisingly found that among the three common SCFAs only butyrate inhibited endothelial NRLP3 inflammasome activation in ECs and prevented the arterial neointima formation in the PLCA model of mice. Acetate and propionate had minimal inhibitory effects on Nlrp3 inflammasome activation and even enhanced the arterial neointima formation in the PLCA model.

We first performed in vivo experiments to test the effects of SCFAs on carotid arterial injury using a mouse model with PLCA. In this model, partial ligation of the carotid artery stimulated vascular inflammation and marked neointima formation [53]. We recently demonstrated that the Nlrp3 inflammasome is importantly involved in the pathological process of the carotid artery in this PLCA mouse model [31]. Our results showed that among three SCFAs, only butyrate significantly decreased Nlrp3 inflammasome formation and activation in the endothelium of ligated carotid arteries in wild type mice, which was comparable to the reduction of Nlrp3 inflammasome activation when the mouse *Asc* gene was deleted. Correspondingly, butyrate significantly abolished the formation of neointima in partially ligated carotid arteries of mice. However, administration of acetate or propionate to mice markedly enhanced the formation and activation of Nlrp3 inflammasome in the carotid arteries with PLCA in $Asc^{+/+}$, but not $Asc^{-/-}$ mice. This Nlrp3 inflammasome activation in wild type mice was accompanied by increased carotid neointima formation during PLCA.

As discussed above, some reported beneficial effects of SCFAs against the development of cardiovascular disease are mainly related to their anti-inflammatory actions, which were observed in different

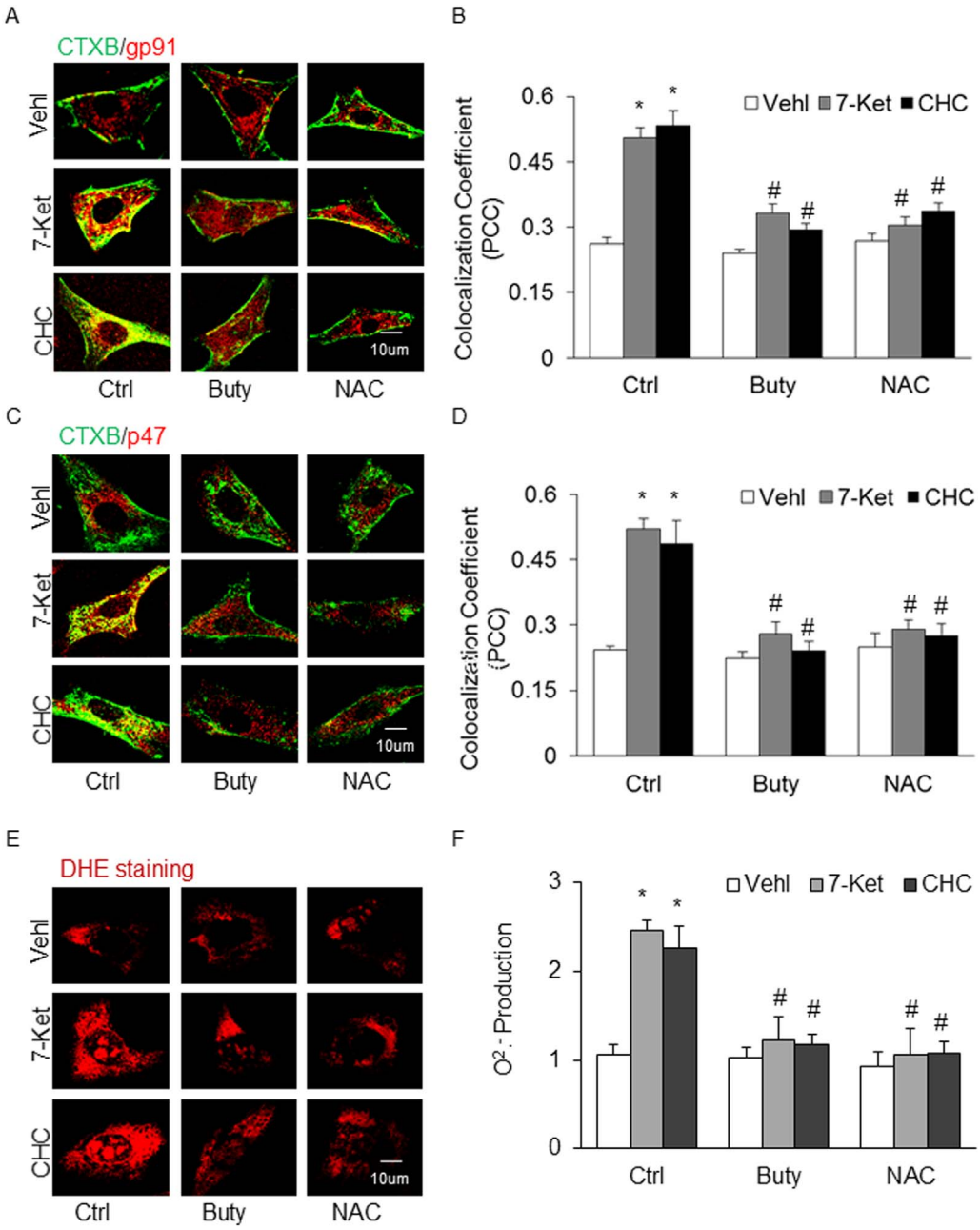

Fig. 8. Effects of Butyrate Associated with Suppression of Lipid raft Redox Signaling Platform Activation. A. Representative fluorescent confocal microscopic images showing the colocalization of LR marker, CTXB with NOX subunit, gp91 (red). B. Summarized data showing PCC of CTXB with gp91 (n = 6). C. Representative fluorescent confocal microscopic images showing the colocalization of LR marker, CTXB with NOX subunit, p47 (red). D. Summarized data showing PCC of CTXB with p47 (n = 5). E. DHE staining showing the representative the cytosolic ROS production. F. NOX-mediated O2·- production as measured by electron spin resonance (ESR) spectrometry (ESR) (n = 5). Data are expressed as means ± SEM. * $p < 0.05$ vs. Vehl group; # $p < 0.05$ vs. Ctrl.

animal models. For example, Wang et al. reported that sodium butyrate treatment can efficiently inhibit Nlrp3 inflammasome activation and thereby inhibits obesity-induced inflammation, indicating that NaB might be a potential anti-inflammatory agent for obesity in db/db mice [24]. In *Ldlr*$^{-/-}$ mice fed on high-cholesterol diet with Nlrp3-deficient or with *Asc*-deficient bone marrow transplantation, plasma levels of inflammatory cytokines such as IL-18 and IL-1 significantly decreased and atherosclerosis induced by high cholesterol was ameliorated [54]. These anti-inflammatory effects of butyrate were also observed in other animal models of vascular inflammation or atherosclerosis such as mice fed the WD, the mouse models of Nlrp3-mediated diseases like Muckle–Wells syndrome, familial cold auto-inflammatory syndrome and urate crystal–induced peritonitis as well as the DSS-induced colitis mouse model [55]. In addition to reduction of inflammatory cytokine production or release, butyrate and other SCFAs were also reported to increase the production of prostaglandin E_2 (PGE_2), an anti-inflammatory prostanoid [56]. Despite these anti-inflammatory effects, SCFAs were also demonstrated to have pro-inflammatory action in some conditions [57]. Several reports have also indicated that SCFAs promote ROS production leading to local tissue oxidative stress enhancing inflammatory response [14,58,59]. The present study demonstrates that the molecular mechanisms by which some SCFAs enhance the innate immune reaction or inflammatory response are due to activation of the intracellular inflammatory machinery, the inflammasome. In tissues with multiple cell types such as the vascular wall, SCFAs may have divergent effects on different cell types, with pro-inflammatory effects on some cell types like macrophages and microglial cells or with anti-inflammatory effects on other cell types such as the inhibitory action of butyrate on ECs [60–62].

Although the present study did not focus on vascular smooth muscle cells (VSMCs), it is well known that both physical and biochemical interactions between ECs and VSMC play a crucial role in vascular homeostasis. ECs may exert regulatory action on VSMC to induce changes in their contractile phenotypes, and in arterial remodeling the interactions of VSMCs with resident vascular cells, extracellular matrix components, and circulating and infiltrating cells are important in the

development of neointima and atherosclerotic plaques. Our previous studies have shown that neointima was inititated by endothelial inflammasome activation, which include VSMCs proliferation, extracellular matrix disturbance, and fibrogenesis [63,64]. It is well known that VCMC phenotypic switch from contractile/differentiated to synthetic/dedifferentiated is essential in the pathogenesis of neointima formation [65]. SCFAs may alter these vascular pathologies during neointima formation via both inflammatory and uncanonical effects of the Nlrp3 inflammasome activation [27,31,66].

To further confirm the effects of SCFAs specifically on ECs and explore related mechanisms, we also performed in vitro experiments in cultured ECs. We first examined the effects of SCFAs on Nlrp3 inflammasome activation induced by 7-Ket and CHC that act directly on the formation and activation of Nlrp3 inflammasomes in ECs. The use of 7-Ket and CHC as atherogenic stimuli is based on previous studies that demonstrated activation of this inflammasome in ECs (EOMA) through different mechanisms [67,68]. It has been reported that 7-Ket as a soluble atherogenic stimulus may activate the Nlrp3 inflammasome through the redox signaling pathway, while CHC activates this inflammasome via crystal particle intrusion or membrane permeability changes to frustrate lysosomes and release cathpsin B [69]. We observed that butyrate significantly decreased the formation and activation of Nlrp3 inflammasomes induced by both 7-Ket and CHC, while propionate only blocked CHC-induced Nlrp3 inflammasome activation. However, acetate had no significant inhibitory effects on Nlrp3 inflammasome activation induced by either 7-Ket or CHC, but itself even activated Nlrp3 inflammsomes in these ECs. Although the present study represents the first study regarding the effects of SCFAs on endothelial Nlrp3 inflammasome activation, the inhibition of Nlrp3 inflammasome activation by butyrate and propionate is consistent with previous findings about the anti-inflammatory action of butyrate and propionate in vascular cells. In this regard, Zapolska-Downar et al. demonstrated that anti-inflammatory and (perhaps) antiatherogenic properties of butyrate may be partially attributed to an effect on the activation of NF-kappaB and PPARα and to associated expression of vascular cell adhesion molecule-1 (VCAM-1) and intracellular cell adhesion molecule-1 (ICAM-1) [70]. Fukae et al. also reported that butyrate may suppress the production of inflammatory mediators by monocytes and macrophages [71]. In human colonic subepithelial myofibroblasts, IFN-γ-induced IP-10 (inducible protein-10) secretion as a type of immune or inflammatory response was also not affected by acetate or propionate, but it was significantly reduced by butyrate [72]. In other studies, propionate and butyrate were found to inhibit the expression of pro-inflammatory mediators (TNF-α, CINC-2αβ and NO) in rat neutrophils, but acetate had no effect [73]. Butyrate and propionate, but not acetate may inhibit the expression of lipopolysaccharide (LPS)-induced production of inflammatory cytokines including neutrophil chemoattractant [55,74,75].

In previous studies, peripheral concentrations of acetate, propionate, and butyrate were detected, which are 19–146, 1–13, and 1–12 μmol/L, respectively [76]. There is a general recognition that acetate is a predominant SCFAs in the blood. Recent studies have investigated its action on cardiovascular diseases, however, little is known about the effects of this SCFA on vascular inflammation. Some studies have indicated that acetate may have pro-inflammatory action, which might be due to its toxicity, rather than its pharmacological or therapeutic effect. The present study showed that acetate even at 100 mM had no toxic effects on cell survival, proliferation or growth (data not show), but it activated Nlrp3 inflammasomes. Similar studies reported that acetic acid in bamboo vinegar was not involved in its anti-inflammatory activity and had no effects on vinegar-induced amelioration of Nlrp3 inflammasome-mediated IL-β increases in LPS- and ATP-activated macrophages [25]. Taken together, it is suggested that only butyrate among the three common SCFAs has anti-inflammatory properties in ECs, which may be attributed to its inhibitory effect on the Nlrp3 inflammasome formation and activation in these cells.

Since SCFAs are generally considered to have beneficial effects on cardiovascular disease, we are particularly interested in the mechanism mediating the inhibitory effects of butyrate on Nlrp3 inflammasome formation and activation. Given that the LR redox signaling platforms were involved in Nlrp3 inflammasome activation [47,77], we determined the contribution of LR redox signaling platform formation and activation induced by 7-Ket and CHC. It was found that butyrate attenuated LR clustering with gp91 or p47 indicating reduction of LR redox signaling platform formation. Direct analysis of $O_2^{\bullet-}$ production in these ECs by DHE staining and ESR spectrometry showed that butyrate blocked 7-Ket or CHC-induced $O_2^{\bullet-}$ production. It seems that butyrate possesses antioxidant action in ECs which may block Nrlp3 inflammasome activation via its redox regulatory domains, such as Nrlp3 binding site to thioredoxin-interacting protein (TXNIP) that is sensitive to redox molecules [78,79]. In previous studies, the activation of the Nlrp3 inflammasome by increased ROS has been reported in different cells [80–82], and NOX and mitochondria-derived ROS may exert an important role [66,82,83]. There is evidence that TXNIP was strongly induced by sodium butyrate and thereby increase caspase 3/7 activation, which may be associated with changes in cell redox status [84]. In addition, butyrate has also been reported to increase the expression of catalase mRNA and proteins in colon epithelium [85] and to protect rat pulmonary artery smooth muscle cells from hypoxia by increasing catalase activity [86]. Taken together, it is possible that butyrate exerts its anti-inflammatory action by inhibition of Nlrp3 inflammasome activation via redox signaling pathway, but it may also work to regulate other cell functions via upregulation of antioxidant enzyme expression and activities such as catalase.

In conclusion, we revealed that SCFAs have differential effects on endothelial Nlrp3 inflammasome activation and associated carotid neointima formation in the arterial wall. Butyrate may have beneficial effects against vascular inflammation or atherosclerosis by its inhibitory action on $O_2^{\bullet-}$ production and consequent Nlrp3 inflammasome formation and activation.

Acknowledgment

This study was supported by grants from the National Institute of Health (HL122937, HL057244 and HL075316).

Appendix A. Supplementary material

Supplementary data associated with this article can be found in the online version at http://dx.doi.org/10.1016/j.redox.2018.02.007.

References

[1] M. McGuire, K.A. Beerman, Nutritional Sciences: from Fundamentals to Food, Wadsworth, Cengage Learning, Belmont, CA, 2013.
[2] A.L. Kau, P.P. Ahern, N.W. Griffin, A.L. Goodman, J.I. Gordon, Human nutrition, the gut microbiome and the immune system, Nature 474 (2011) 327–336.
[3] H.V. Lin, A. Frassetto, E.J. Kowalik Jr., A.R. Nawrocki, M.M. Lu, J.R. Kosinski, J.A. Hubert, D. Szeto, X. Yao, G. Forrest, D.J. Marsh, Butyrate and propionate protect against diet-induced obesity and regulate gut hormones via free fatty acid receptor 3-independent mechanisms, PLoS One 7 (2012) e35240.
[4] E.N. Bergman, Energy contributions of volatile fatty acids from the gastrointestinal tract in various species, Physiol. Rev. 70 (1990) 567–590.
[5] J.H. Cummings, G.T. Macfarlane, The control and consequences of bacterial fermentation in the human colon, J. Appl. Bacteriol. 70 (1991) 443–459.
[6] G.T. Macfarlane, S. Macfarlane, Fermentation in the human large intestine: its physiologic consequences and the potential contribution of prebiotics, J. Clin. Gastroenterol. 45 (Suppl:S120–127) (2011).
[7] A.A. Salyers, Energy sources of major intestinal fermentative anaerobes, Am. J. Clin. Nutr. 32 (1979) 158–163.
[8] D.R. Donohoe, N. Garge, X. Zhang, W. Sun, T.M. O'Connell, M.K. Bunger, S.J. Bultman, The microbiome and butyrate regulate energy metabolism and autophagy in the mammalian colon, Cell Metab. 13 (2011) 517–526.
[9] L.V. Hooper, J.I. Gordon, Commensal host-bacterial relationships in the gut, Science 292 (2001) 1115–1118.
[10] I.R. Sanderson, Nutritional factors and immune functions of gut epithelium, Proc. Nutr. Soc. 60 (2001) 443–447.

[11] L. Biancone, I. Monteleone, G. Del Vecchio Blanco, P. Vavassori, F. Pallone, Resident bacterial flora and immune system, Dig. Liver Dis. 34 (Suppl 2) (2002) S37–S43.
[12] C. De Filippo, D. Cavalieri, M. Di Paola, M. Ramazzotti, J.B. Poullet, S. Massart, S. Collini, G. Pieraccini, P. Lionetti, Impact of diet in shaping gut microbiota revealed by a comparative study in children from Europe and rural Africa, Proc. Natl. Acad. Sci. USA 107 (2010) 14691–14696.
[13] J.M. Uronis, M. Muhlbauer, H.H. Herfarth, T.C. Rubinas, G.S. Jones, C. Jobin, Modulation of the intestinal microbiota alters colitis-associated colorectal cancer susceptibility, PLoS One 4 (2009) e6026.
[14] K.M. Maslowski, A.T. Vieira, A. Ng, J. Kranich, F. Sierro, D. Yu, H.C. Schilter, M.S. Rolph, F. Mackay, D. Artis, R.J. Xavier, M.M. Teixeira, C.R. Mackay, Regulation of inflammatory responses by gut microbiota and chemoattractant receptor GPR43, Nature 461 (2009) 1282–1286.
[15] M. Vijay-Kumar, J.D. Aitken, F.A. Carvalho, T.C. Cullender, S. Mwangi, S. Srinivasan, S.V. Sitaraman, R. Knight, R.E. Ley, A.T. Gewirtz, Metabolic syndrome and altered gut microbiota in mice lacking Toll-like receptor 5, Science 328 (2010) 228–231.
[16] S. Mariathasan, K. Newton, D.M. Monack, D. Vucic, D.M. French, W.P. Lee, M. Roose-Girma, S. Erickson, V.M. Dixit, Differential activation of the inflammasome by caspase-1 adaptors ASC and Ipaf, Nature 430 (2004) 213–218.
[17] R. Zhou, A. Tardivel, B. Thorens, I. Choi, J. Tschopp, Thioredoxin-interacting protein links oxidative stress to inflammasome activation, Nat. Immunol. 11 (2010) 136–140.
[18] R.A. Ratsimandresey, A. Dorfleutner, C. Stehlik, An update on PYRIN domain-containing pattern recognition receptors: from immunity to pathology, Front Immunol. 4 (2013) 440.
[19] Y. Chen, A.L. Pitzer, X. Li, P.L. Li, L. Wang, Y. Zhang, Instigation of endothelial Nlrp3 inflammasome by adipokine visfatin promotes inter-endothelial junction disruption: role of HMGB1, J. Cell. Mol. Med. 19 (2015) 2715–2727.
[20] T. Strowig, J. Henao-Mejia, E. Elinav, R. Flavell, Inflammasomes in health and disease, Nature 481 (2012) 278–286.
[21] F. Martinon, K. Burns, J. Tschopp, The inflammasome: a molecular platform triggering activation of inflammatory caspases and processing of proIL-beta, Mol. Cell 10 (2002) 417–426.
[22] A.B. Imaeda, A. Watanabe, M.A. Sohail, S. Mahmood, M. Mohamadnejad, F.S. Sutterwala, R.A. Flavell, W.Z. Mehal, Acetaminophen-induced hepatotoxicity in mice is dependent on Tlr9 and the Nalp3 inflammasome, J. Clin. Investig. 119 (2009) 305–314.
[23] F. Martinon, V. Petrilli, A. Mayor, A. Tardivel, J. Tschopp, Gout-associated uric acid crystals activate the NALP3 inflammasome, Nature 440 (2006) 237–241.
[24] X. Wang, G. He, Y. Peng, W. Zhong, Y. Wang, B. Zhang, Sodium butyrate alleviates adipocyte inflammation by inhibiting NLRP3 pathway, Sci. Rep. 5 (2015) 12676.
[25] C.L. Ho, C.Y. Lin, S.M. Ka, A. Chen, Y.L. Tasi, M.L. Liu, Y.C. Chiu, K.F. Hua, Bamboo vinegar decreases inflammatory mediator expression and NLRP3 inflammasome activation by inhibiting reactive oxygen species generation and protein kinase C-alpha/delta activation, PLoS One 8 (2013) e75738.
[26] Y.H. Youm, K.Y. Nguyen, R.W. Grant, E.L. Goldberg, M. Bodogai, D. Kim, D. D'Agostino, N. Planavsky, C. Lupfer, T.D. Kanneganti, S. Kang, T.L. Horvath, T.M. Fahmy, P.A. Crawford, A. Biragyn, E. Alnemri, V.D. Dixit, The ketone metabolite beta-hydroxybutyrate blocks NLRP3 inflammasome-mediated inflammatory disease, Nat. Med. 21 (2015) 263–269.
[27] Y. Zhang, J. Wang, H. Li, L. Yuan, L. Wang, B. Wu, J. Ge, Hydrogen sulfide suppresses transforming growth factor-beta1-induced differentiation of human cardiac fibroblasts into myofibroblasts, Sci. China Life Sci. 58 (2015) 1126–1134.
[28] D. Nam, C.W. Ni, A. Rezvan, J. Suo, K. Budzyn, A. Llanos, D. Harrison, D. Giddens, H. Jo, Partial carotid ligation is a model of acutely induced disturbed flow, leading to rapid endothelial dysfunction and atherosclerosis, Am. J. Physiol. Heart Circ. Physiol. 297 (2009) H1535–H1543.
[29] V.A. Korshunov, B.C. Berk, Flow-induced vascular remodeling in the mouse: a model for carotid intima-media thickening, Arterioscler. Thromb. Vasc. Biol. 23 (2003) 2185–2191.
[30] N. Yajima, M. Takahashi, H. Morimoto, Y. Shiba, Y. Takahashi, J. Masumoto, H. Ise, J. Sagara, J. Nakayama, S. Taniguchi, U. Ikeda, Critical role of bone marrow apoptosis-associated speck-like protein, an inflammasome adaptor molecule, in neointimal formation after vascular injury in mice, Circulation 117 (2008) 3079–3087.
[31] M. Xia, K.M. Boini, J.M. Abais, M. Xu, Y. Zhang, P.L. Li, Endothelial NLRP3 inflammasome activation and enhanced neointima formation in mice by adipokine visfatin, Am. J. Pathol. 184 (2014) 1617–1628.
[32] N.G. Abraham, K. Sodhi, A.M. Silvis, L. Vanella, G. Favero, R. Rezzani, C. Lee, D.C. Zeldin, M.L. Schwartzman, CYP2J2 targeting to endothelial cells attenuates adiposity and vascular dysfunction in mice fed a high-fat diet by reprogramming adipocyte phenotype, Hypertension 64 (2014) 1352–1361.
[33] I.J. Shin, S.M. Shon, D. Schellingerhout, J.Y. Park, J.Y. Kim, S.K. Lee, D.K. Lee, H.W. Lee, B.C. Ahn, K. Kim, I.C. Kwon, D.E. Kim, Characterization of partial ligation-induced carotid atherosclerosis model using dual-modality molecular imaging in ApoE knock-out mice, PLoS One 8 (2013) e73451.
[34] D. Nam, C.W. Ni, A. Rezvan, J. Suo, K. Budzyn, A. Llanos, D.G. Harrison, D.P. Giddens, H. Jo, A model of disturbed flow-induced atherosclerosis in mouse carotid artery by partial ligation and a simple method of RNA isolation from carotid endothelium, J. Vis. Exp. (2010).
[35] G. Lee, J.H. Shim, H. Kang, K.M. Nam, H. Song, J.T. Park, Monodisperse Pt and PtRu/C(60) hybrid nanoparticles for fuel cell anode catalysts, Chem. Commun. (2009) 5036–5038.
[36] G. Frost, M.L. Sleeth, M. Sahuri-Arisoylu, B. Lizarbe, S. Cerdan, L. Brody, J. Anastasovska, S. Ghourab, M. Hankir, S. Zhang, D. Carling, J.R. Swann, G. Gibson, A. Viardot, D. Morrison, E. Louise Thomas, J.D. Bell, The short-chain fatty acid acetate reduces appetite via a central homeostatic mechanism, Nat. Commun. 5 (2014) 3611.
[37] H.J. Kim, M. Rowe, M. Ren, J.S. Hong, P.S. Chen, D.M. Chuang, Histone deacetylase inhibitors exhibit anti-inflammatory and neuroprotective effects in a rat permanent ischemic model of stroke: multiple mechanisms of action, J. Pharmacol. Exp. Ther. 321 (2007) 892–901.
[38] M. Xia, C. Zhang, K.M. Boini, A.M. Thacker, P.L. Li, Membrane raft-lysosome redox signalling platforms in coronary endothelial dysfunction induced by adipokine visfatin, Cardiovasc. Res. 89 (2011) 401–409.
[39] C. Zhang, F. Yi, M. Xia, K.M. Boini, Q. Zhu, L.A. Laperle, J.M. Abais, C.A. Brimson, P.L. Li, NMDA receptor-mediated activation of NADPH oxidase and glomerulosclerosis in hyperhomocysteinemic rats, Antioxid. Redox Signal 13 (2010) 975–986.
[40] M. Xu, X.X. Li, L. Wang, M. Wang, Y. Zhang, P.L. Li, Contribution of Nrf2 to atherogenic phenotype switching of coronary arterial smooth muscle cells lacking CD38 gene, Cell Physiol. Biochem. 37 (2015) 432–444.
[41] A.Y. Zhang, F. Yi, G. Zhang, E. Gulbins, P.L. Li, Lipid raft clustering and redox signaling platform formation in coronary arterial endothelial cells, Hypertension 47 (2006) 74–80.
[42] X. Xu, A. Zhang, N. Li, P.L. Li, F. Zhang, Concentration-dependent diversifcation effects of free cholesterol loading on macrophage viability and polarization, Cell Physiol. Biochem. 37 (2015) 419–431.
[43] Y. Zhang, X. Li, A.L. Pitzer, Y. Chen, L. Wang, P.L. Li, Coronary endothelial dysfunction induced by nucleotide oligomerization domain-like receptor protein with pyrin domain containing 3 inflammasome activation during hypercholesterolemia: beyond inflammation, Antioxid. Redox Signal 22 (2015) 1084–1096.
[44] A. Gomes, E. Fernandes, J.L. Lima, Fluorescence probes used for detection of reactive oxygen species, J. Biochem. Biophys. Methods 65 (2005) 45–80.
[45] B. Kalyanaraman, V. Darley-Usmar, K.J. Davies, P.A. Dennery, H.J. Forman, M.B. Grisham, G.E. Mann, K. Moore, L.J. Roberts 2nd, H. Ischiropoulos, Measuring reactive oxygen and nitrogen species with fluorescent probes: challenges and limitations, Free Radic. Biol. Med. 52 (2012) 1–6.
[46] S. Karimi-Abdolrezaee, D. Schut, J. Wang, M.G. Fehlings, Chondroitinase and growth factors enhance activation and oligodendrocyte differentiation of endogenous neural precursor cells after spinal cord injury, Plos One 7 (2012) e37589.
[47] C. Zhang, K.M. Boini, M. Xia, J.M. Abais, X. Li, Q. Liu, P.L. Li, Activation of Nod-like receptor protein 3 inflammasomes turns on podocyte injury and glomerular sclerosis in hyperhomocysteinemia, Hypertension 60 (2012) 154–162.
[48] G. Favero, C. Paganelli, B. Buffoli, L.F. Rodella, R. Rezzani, Endothelium and its alterations in cardiovascular diseases: life style intervention, BioMed. Res. Int. 2014 (2014) 801896.
[49] S. Hussain, S. Sangtian, S.M. Anderson, R.J. Snyder, J.D. Marshburn, A.B. Rice, J.C. Bonner, S. Garantziotis, Inflammasome activation in airway epithelial cells after multi-walled carbon nanotube exposure mediates a profibrotic response in lung fibroblasts, Part. Fibre Toxicol. 11 (2014) 28.
[50] M.J. Kennedy, K.D. Jellerson, M.Z. Snow, M.L. Zacchetti, Challenges in the pharmacologic management of obesity and secondary dyslipidemia in children and adolescents, Paediatr. Drugs 15 (2013) 335–342.
[51] S.M. Grundy, J.I. Cleeman, S.R. Daniels, K.A. Donato, R.H. Eckel, B.A. Franklin, D.J. Gordon, R.M. Krauss, P.J. Savage, S.C. Smith Jr., J.A. Spertus, F. Costa, Diagnosis and management of the metabolic syndrome: an American Heart Association/National Heart, Lung, and Blood Institute Scientific Statement, Circulation 112 (2005) 2735–2752.
[52] P.A. Ades, P.D. Savage, Potential benefits of weight loss in coronary heart disease, Progress. Cardiovasc. Dis. 56 (2014) 448–456.
[53] N. Alberts-Grill, A. Rezvan, D.J. Son, H. Qiu, C.W. Kim, M.L. Kemp, C.M. Weyand, H. Jo, Dynamic immune cell accumulation during flow-induced atherogenesis in mouse carotid artery: an expanded flow cytometry method, Arterioscler. Thromb Vasc. Biol. 32 (2012) 623–632.
[54] P. Duewell, H. Kono, K.J. Rayner, C.M. Sirois, G. Vladimer, F.G. Bauernfeind, G.S. Abela, L. Franchi, G. Nunez, M. Schnurr, T. Espevik, E. Lien, K.A. Fitzgerald, K.L. Rock, K.J. Moore, S.D. Wright, V. Hornung, E. Latz, NLRP3 inflammasomes are required for atherogenesis and activated by cholesterol crystals, Nature 464 (2010) 1357–1361.
[55] J. Ji, D. Shu, M. Zheng, J. Wang, C. Luo, Y. Wang, F. Guo, X. Zou, X. Lv, Y. Li, T. Liu, H. Qu, Microbial metabolite butyrate facilitates M2 macrophage polarization and function, Sci. Rep. 6 (2016) 24838.
[56] M.A. Cox, J. Jackson, M. Stanton, A. Rojas-Triana, L. Bober, M. Laverty, X.X. Yang, F. Zhu, J.J. Liu, S.K. Wang, F. Monsma, G. Vassileva, M. Maguire, E. Gustafson, M. Bayne, C.C. Chou, D. Lundell, C.H. Jenh, Short-chain fatty acids act as antiinflammatory mediators by regulating prostaglandin E-2 and cytokines, World J. Gastroentero 15 (2009) 5549–5557.
[57] M.A. Vinolo, H.G. Rodrigues, E. Hatanaka, C.B. Hebeda, S.H. Farsky, R. Curi, Short-chain fatty acids stimulate the migration of neutrophils to inflammatory sites, Clin. Sci. 117 (2009) 331–338.
[58] R.E. Stringer, C.A. Hart, S.W. Edwards, Sodium butyrate delays neutrophil apoptosis: role of protein biosynthesis in neutrophil survival, Br. J. Haematol. 92 (1996) 169–175.
[59] S. Nakao, Y. Moriya, S. Furuyama, R. Niederman, H. Sugiya, Propionic acid stimulates superoxide generation in human neutrophils, Cell Biol. Int. 22 (1998) 331–337.
[60] J. Huuskonen, T. Suuronen, T. Nuutinen, S. Kyrylenko, A. Salminen, Regulation of microglial inflammatory response by sodium butyrate and short-chain fatty acids, Br. J. Pharmacol. 141 (2004) 874–880.
[61] E. Bailon, M. Cueto-Sola, P. Utrilla, M.E. Rodriguez-Cabezas, N. Garrido-Mesa,

A. Zarzuelo, J. Xaus, J. Galvez, M. Comalada, Butyrate in vitro immune-modulatory effects might be mediated through a proliferation-related induction of apoptosis, Immunobiology 215 (2010) 863–873.
[62] M.A. Halili, M.R. Andrews, L.I. Labzin, K. Schroder, G. Matthias, C. Cao, E. Lovelace, R.C. Reid, G.T. Le, D.A. Hume, K.M. Irvine, P. Matthias, D.P. Fairlie, M.J. Sweet, Differential effects of selective HDAC inhibitors on macrophage inflammatory responses to the Toll-like receptor 4 agonist LPS, J. Leukoc. Biol. 87 (2010) 1103–1114.
[63] C.A. Mason, P. Chang, C. Fallery, M. Rabinovitch, Nitric oxide mediates LC-3-dependent regulation of fibronectin in ductus arteriosus intimal cushion formation, FASEB J. 13 (1999) 1423–1434.
[64] R.I. Clyman, S.R. Seidner, H. Kajino, C. Roman, C.J. Koch, N. Ferrara, N. Waleh, F. Mauray, Y.Q. Chen, E.A. Perkett, T. Quinn, VEGF regulates remodeling during permanent anatomic closure of the ductus arteriosus, Am. J. Physiol. Regul. Integr. Comp. Physiol. 282 (2002) R199–R206.
[65] N. Shi, S.Y. Chen, Smooth muscle cell differentiation: model systems, regulatory mechanisms, and vascular diseases, J. Cell Physiol. 231 (2016) 777–787.
[66] J.M. Abais, M. Xia, Y. Zhang, K.M. Boini, P.L. Li, Redox regulation of NLRP3 inflammasomes: ROS as trigger or effector? Antioxid. Redox Signal 22 (2015) 1111–1129.
[67] M. Xia, K. Boini, Y. Chen, Y. Zhang, P.L. Li, Activation of endothelial NLRP3 Inflammasomes associated with acid sphingomyelinase-dependent formation of membrane Raft redox signaling platforms, Faseb J. 29 (2015).
[68] X. Li, Y. Zhang, M. Xia, E. Gulbins, K.M. Boini, P.L. Li, Activation of Nlrp3 inflammasomes enhances macrophage lipid-deposition and migration: implication of a novel role of inflammasome in atherogenesis, PloS One 9 (2014).
[69] K. Rajamaki, J. Lappalainen, K. Oorni, E. Valimaki, S. Matikainen, P.T. Kovanen, K.K. Eklund, Cholesterol crystals activate the NLRP3 inflammasome in human macrophages: a novel link between cholesterol metabolism and inflammation, PloS One 5 (2010) e11765.
[70] D. Zapolska-Downar, A. Siennicka, M. Kaczmarczyk, B. Kolodziej, M. Naruszewicz, Butyrate inhibits cytokine-induced VCAM-1 and ICAM-1 expression in cultured endothelial cells: the role of NF-kappaB and PPARalpha, J. Nutr. Biochem. 15 (2004) 220–228.
[71] J. Fukae, Y. Amasaki, Y. Yamashita, T. Bohgaki, S. Yasuda, S. Jodo, T. Atsumi, T. Koike, Butyrate suppresses tumor necrosis factor alpha production by regulating specific messenger RNA degradation mediated through a cis-acting AU-rich element, Arthritis Rheum. 52 (2005) 2697–2707.
[72] O. Inatomi, A. Andoh, K. Kitamura, H. Yasui, Z. Zhang, Y. Fujiyama, Butyrate blocks interferon-gamma-inducible protein-10 release in human intestinal subepithelial myofibroblasts, J. Gastroenterol. 40 (2005) 483–489.
[73] M.A. Vinolo, H.G. Rodrigues, E. Hatanaka, F.T. Sato, S.C. Sampaio, R. Curi, Suppressive effect of short-chain fatty acids on production of proinflammatory mediators by neutrophils, J. Nutr. Biochem. 22 (2011) 849–855.
[74] C. Nastasi, M. Candela, C.M. Bonefeld, C. Geisler, M. Hansen, T. Krejsgaard, E. Biagi, M.H. Andersen, P. Brigidi, N. Odum, T. Litman, A. Woetmann, The effect of short-chain fatty acids on human monocyte-derived dendritic cells, Sci. Rep. 5 (2015) 16148.
[75] C. Iraporda, A. Errea, D.E. Romanin, D. Cayet, E. Pereyra, O. Pignataro, J.C. Sirard, G.L. Garrote, A.G. Abraham, M. Rumbo, Lactate and short chain fatty acids produced by microbial fermentation downregulate proinflammatory responses in intestinal epithelial cells and myeloid cells, Immunobiology 220 (2015) 1161–1169.
[76] J.H. Cummings, E.W. Pomare, W.J. Branch, C.P. Naylor, G.T. Macfarlane, Short chain fatty acids in human large intestine, portal, hepatic and venous blood, Gut 28 (1987) 1221–1227.
[77] J.M. Abais, C. Zhang, M. Xia, Q. Liu, T.W. Gehr, K.M. Boini, P.L. Li, NADPH oxidase-mediated triggering of inflammasome activation in mouse podocytes and glomeruli during hyperhomocysteinemia, Antioxid. Redox Signal. 18 (2013) 1537–1548.
[78] J.M. Abais, M. Xia, G. Li, Y. Chen, S.M. Conley, T.W. Gehr, K.M. Boini, P.L. Li, Nod-like receptor protein 3 (NLRP3) inflammasome activation and podocyte injury via thioredoxin-interacting protein (TXNIP) during hyperhomocysteinemia, J. Biol. Chem. 289 (2014) 27159–27168.
[79] J.M. Abais, M. Xia, G. Li, T.W. Gehr, K.M. Boini, P.L. Li, Contribution of endogenously produced reactive oxygen species to the activation of podocyte NLRP3 inflammasomes in hyperhomocysteinemia, Free Radic. Biol. Med. 67 (2014) 211–220.
[80] K. Wang, Y. Yao, X. Zhu, K. Zhang, F. Zhou, L. Zhu, Amyloid beta induces NLRP3 inflammasome activation in retinal pigment epithelial cells via NADPH oxidase- and mitochondria-dependent ROS production, J. Biochem. Mol. Toxicol. (2017) 31.
[81] R. von Bernhardi, L. Eugenin-von Bernhardi, J. Eugenin, Microglial cell dysregulation in brain aging and neurodegeneration, Front. Aging Neurosci. 7 (2015) 124.
[82] S.R. Kim, D.I. Kim, S.H. Kim, H. Lee, K.S. Lee, S.H. Cho, Y.C. Lee, NLRP3 inflammasome activation by mitochondrial ROS in bronchial epithelial cells is required for allergic inflammation, Cell Death Dis. 5 (2014) e1498.
[83] W. Ding, H. Guo, C. Xu, B. Wang, M. Zhang, F. Ding, Mitochondrial reactive oxygen species-mediated NLRP3 inflammasome activation contributes to aldosterone-induced renal tubular cells injury, Oncotarget 7 (2016) 17479–17491.
[84] X. Jin, N. Wu, J. Dai, Q. Li, X. Xiao, TXNIP mediates the differential responses of A549 cells to sodium butyrate and sodium 4-phenylbutyrate treatment, Cancer Med. 6 (2017) 424–438.
[85] F. Jahns, A. Wilhelm, N. Jablonowski, H. Mothes, K.O. Greulich, M. Glei, Butyrate modulates antioxidant enzyme expression in malignant and non-malignant human colon tissues, Mol. Carcinog. 54 (2015) 249–260.
[86] S. Yano, D.F. Tierney, Butyrate increases catalase activity and protects rat pulmonary artery smooth muscle cells against hyperoxia, Biochem. Biophys. Res. Commun. 164 (1989) 1143–1148.